Pergamon

Journal of Terramechanics, Vol. 33, No. 1, pp. 1–11, 1996
Published by Elsevier Science Ltd

0022-4898/96 $15.00 + 0.00

PII:S0022-4898(96)00004-3

SOIL STRESSES UNDER A TRACTOR TIRE AT VARIOUS LOADS AND INFLATION PRESSURES*

A. C. BAILEY†, R. L. RAPER†, T. R. WAY†, E.C. BURT† and C. E. JOHNSON††

Summary—Soil stresses were measured under a 18.4R38 R-1 radial-ply tractor tire, operated at two levels each of dynamic load and inflation pressure. Stress state transducers were placed at two depths beneath the centerline of the path of the tractor tire in two different compaction profiles in each of two soils. Peak soil stresses and soil bulk density increased with increases in both dynamic load and inflation pressure. Copyright © 1996 ISTVS. Published by Elsevier Science Ltd.

INTRODUCTION

In 1992, as a solution to the problem of 'power hop', tractor and tire manufacturers presented revised load and inflation pressure tables for radial-ply drive wheel tractor tires [1–3]. Power hop, a jumping or bouncing of the tractor creating a very uncomfortable ride and dangerous loss of traction and operator control during field operations, had been a nagging problem for the machinery and tire industries since the introduction of radial-ply tires and four-wheel drive tractors. Previously, the only immediate solution to control power hop in the field was to change either the draft load or ground speed. The new industry recommendations allowed inflation pressures in radial-ply tires to be set as low as 41 kPa (6 psi) as long as the load on the tire was suitable. Previous tables went no lower than 83 kPa (12 psi). Customers were encouraged to use larger tires and the new minimum inflation pressures on four-wheel drive tractors [4, 5]. Other advantages to be achieved, however, from using lower inflation pressure included improved traction, flotation, ride, stability and less soil compaction [2].

These new tractor drive tire load and inflation pressure tables presented a unique opportunity to study load–inflation pressure interactions. Tractor tire load ratings are paired values of load and inflation pressures which yield approximately the same deflection of the tire on a rigid surface. Thus, all load–inflation pressure combinations for a given tire represent approximately the same deflection of that tire and hence, the same contact area, on a rigid surface [2]. Goodyear [2] lists the rated load range of an 18.4R38 tire to be 13.2 kN (2960 lb) at 41.4 kPa (6 psi) and 25.3 kN (5680 lb) at 124 kPa (18 psi). The load increases by a factor of 1.9 and the inflation pressure increases by a factor of three, all at a nominally constant contact area.

Both dynamic load (total normal force exerted by a tire on the soil, including static load and load transfer) and inflation pressure are important factors in the performance

†USDA, ARS, National Soil Dynamics Laboratory, Auburn, AL, U.S.A.
††Agricultural Engineering Dept., Alabama Agricultural Experiment Station, Auburn University, AL, U.S.A.

of tractor tires [6, 7]. There is also evidence that dynamic load affects soil stresses under the tractor tire [8]. The effect of inflation pressure is less clear. Bailey *et al.* [9] concluded that tire inflation pressure affected soil stresses under the tire in sandy soils. However, their data from a clay loam soil did not statistically support a similar conclusion. Earlier research by Bailey *et al.* [10] found no effect of inflation pressure on soil stresses in a silt loam soil.

The primary objective of this study was to investigate changes in the soil stress state caused by the operation of a tractor tire at each of two different levels of load and inflation pressure. Two of the four combinations were at the manufacturer's recommendation for load and inflation pressure, the other two were an 'over-inflated' combination in which the inflation pressure was higher than that required for the load, and an 'under-inflated' condition in which the inflation pressure was less than that required for the load. A secondary objective was to determine if inflation pressure alone affected soil stresses generated beneath the tire.

EXPERIMENTAL PROCEDURE

This study used the stress state transducers (SST) described by Nichols *et al.* [11] and is shown in Fig. 1. These SSTs provide the data necessary to calculate the complete stress state at the transducer [12]. The stress state is a 3 × 3 symmetric tensor with six independent stresses, and may be represented by three normal stresses (σ_x, σ_y, σ_z) and three shear stresses (τ_{xy}, τ_{xz}, and τ_{yz}) with respect to any arbitrary x, y, z directions not in the directions of the principal stresses. Calculation of the stress state requires the measurement of six unique pressures from which one can calculate σ_x, σ_y, σ_z, τ_{xy}, τ_{xz}, and τ_{yz}. The SSTs described by Nichols *et al.* [11] used small commercially-available pressure transducers to

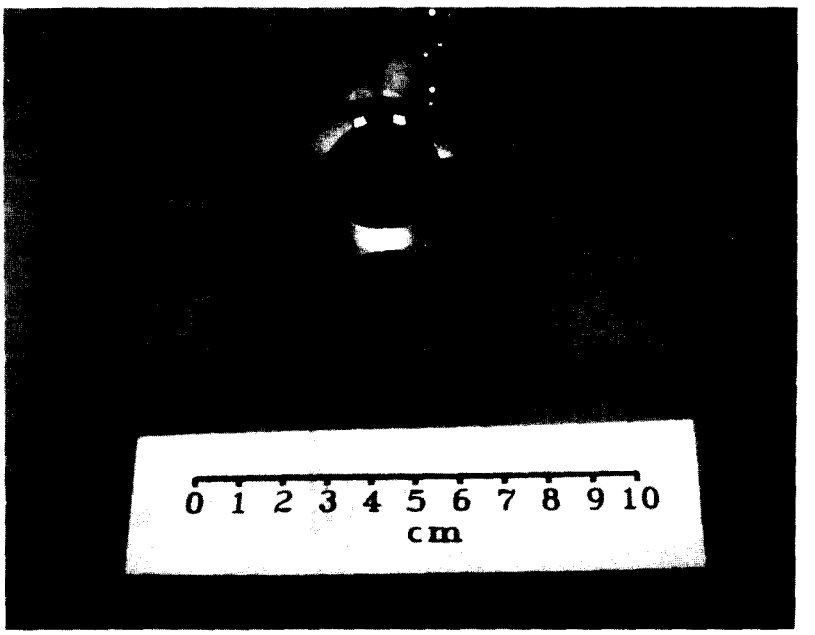

Fig. 1. A soil stress state transducer.

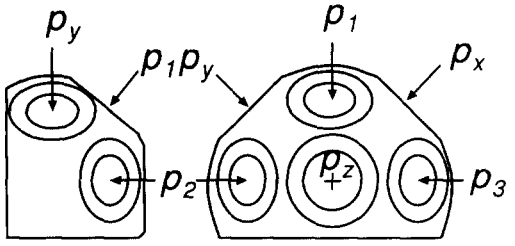

Fig. 2. Schematic of the soil stress state transducer.

measure the normal pressure acting on six unique planes. Three of the planes were mutually orthogonal (the planes of p_x, p_y, and p_z) and three were non-orthogonal (the planes of p_1, p_2, and p_3) (Fig. 2). The directions of the three non-orthogonal planes were chosen to keep all six pressure sensors in close proximity and provide a balanced contribution in the calculation of the shear stresses acting on the x, y and z planes. The shear stresses can be calculated from the six measured pressures (p_x, p_y, p_z, p_1, p_2, and p_3) and the direction cosines of the planes of p_1, p_2, and p_3, either 0.5774 or –0.5774 with respect to the x, y, and z axes, using the following equations:

$$\begin{aligned} \tau_{xy} &= -0.75\,(p_2 + p_3) + 0.5\,(p_x + p_y + p_z); \\ \tau_{xz} &= 0.75\,(p_1 + p_3) - 0.5\,(p_x + p_y + p_z); \text{ and} \\ \tau_{yz} &= 0.75\,(p_1 + p_2) - 0.5\,(p_x + p_y + p_z). \end{aligned} \tag{1}$$

Once these three shear stresses are determined, the tensor is complete and may be solved for the eigenvalues (principal stresses σ_1, σ_2, σ_3). Other stresses on particular planes can then be calculated, such as the octahedral normal (σ_{oct}):

$$\sigma_{oct} = (\sigma_1 + \sigma_2 + \sigma_3) / 3 \tag{2}$$

and shear (τ_{oct}) stresses:

$$\tau_{oct} = \sqrt{(\sigma_1 - \sigma_2)^2 + (\sigma_2 - \sigma_3)^2 + (\sigma_3 - \sigma_1)^2} / 3. \tag{3}$$

The major principal stress, σ_1, is the greatest compressive stress. Previous work by Bailey *et al.* [10] however, found that σ_1 displays the same trends as the octahedral shear stress. For this discussion the octahedral stresses σ_{oct} and τ_{oct} will be used to represent the stress state in the soil under the tractor tire.

This experiment was conducted in the soil bins of the National Soil Dynamics Laboratory (NSDL), a facility of the Agricultural Research Service, United States Department of Agriculture in Auburn, Alabama, USA. The tire used in this experiment was a Goodyear* 18.4R38 Dyna Torque Radial (2 star) R-1 tire, and was operated by the NSDL's single wheel traction research vehicle in the soil bins. Burt *et al.* [13] have described the single wheel traction research vehicle, and the NSDL data acquisition and control

*Mention of trade marks or company name does not imply endorsement of these products by USDA or Auburn University.

system has been described by Lyne *et al.* [14]. A forward velocity of 0.15 m/s and 10% slip were used for all tests. All operating parameters were held constant within a test run.

The treatments in this experiment were different combinations of load and inflation pressure, and are presented in Table 1. Treatments *L* (low, 13.2 kN dynamic load-41.4 kPa inflation pressure) and *H* (high, 25.3 kN dynamic load-124 kPa inflation pressure) were two combinations of load and inflation pressure taken from the manufacturer's tables [2]. The *O* (over-inflated, 13.2 kN dynamic load-124 kPa inflation pressure) treatment used the load from the *L* level (13.2 kN) and the inflation pressure from the *H* treatment (124 kPa), and was so named because the tire is 'over inflated' at that dynamic load. The *U* (under-inflated, 25.3 kN dynamic load-41.4 kPa inflation pressure) treatment used the load from the *H* level (25.3 kN) and the inflation pressure of the *L* treatment (41.4 kPa). The tire is under-inflated at this level of dynamic load. The treatment labels *O* and *U* are reversed from earlier usage by Bailey *et al.* [15].

The load of 25.3 kN used in the under-inflated *U* treatment greatly exceeds manufacturer's recommendation for load for the 41.4 kPa inflation pressure, and is not recommended for field operations. However, it was thought that the tire could withstand this overload for short periods of time because of the very low operating speeds and short, straight travel distances involved in this research situation. Also, the manufacturer's load tables are for static loads, whereas the NSDL single wheel traction research vehicle controls the actual dynamic load and inflation pressure. Thus, a tire inflated to the recommended inflation pressure for the static load of a given tractor may actually operate at higher dynamic loads in the field because of load transfer. All of the load treatments in this experiment were probably lower than what would be found in field situations because load transfer occurs in most field operations. In this respect, the under-inflated treatment *U* may not be quite as extreme as it seems.

The experiment was conducted in the NSDL's two indoor soil bins. One bin contained a Norfolk sandy loam (NSL) (*Typic paleudults*) and the other bin contained a Decatur clay loam (DCL) (*Rhodic paleudults*). Both soil bins were prepared twice to obtain two different density profiles. For one profile in each soil, the soil was rotary tilled to a depth of approximately 600 mm. Then a hardpan was established over the entire soil bin using a single moldboard plow with a trailing steel wheel operating in the plow furrow. The loose soil above the hardpan was then leveled. The top of the hardpan was approximately 410 mm below the loose surface of the NSL and 300 mm below the surface of the DCL. This soil profile will be referred to as the 'hardpan profile'. The second profile in each soil was prepared with the same procedure except that no hardpan was created. The soil was left in a relatively uniform profile. This soil condition will be referred to as the 'uniform profile'. The initial conditions for both soils and profiles, taken immediately above the hardpan or at a corresponding depth in the uniform profile, are presented in Table 2.

Table 1. Load–inflation pressure combinations

Treatment	Load		Inflation pressure	
	Level	kN	Level	kPa
L	1	13.2	1	41.4
O	1	13.2	2	124.0
U	2	25.3	1	41.4
H	2	25.3	2	124.0

Table 2. Soil initial conditions 10–50 mm above hardpan (if present)

Soil	Profile	Moisture content % d.b.	Bulk density Mg/m^3	Cone index MPa
NSL	uniform	7.6	1.189	0.94
NSL	hardpan	7.1	1.321	0.72
DCL	uniform	13.4	1.081	1.26
DCL	hardpan	12.9	1.098	0.98

There was enough length in the soil bins for four replications of each treatment. Each bin was divided into four blocks (replications) and all treatments were conducted in one block at a time. The blocks not being used were covered with a plastic sheet to minimize soil moisture changes during the testing procedure.

The two SSTs used in the study were placed at different depths under the centerline of the path of the tire with a horizontal spacing of 0.5 m. One SST was placed immediately above the hardpan or at the same depth if no hardpan was present. This will be referred to as the 'hardpan depth'. The top of the SST at this depth was approximately 355 mm below the loose surface of the NSL and 245 mm below the surface of the DCL. The second SST was placed at a depth between the surface and the hardpan depth. This will be referred to as the 'shallow depth'. The top of the SST at the shallow depth was 260 mm in the NSL and 210 mm in the DCL.

Soil bulk density samples were taken beneath each tire track at the final depth of each SST. Bulk density was analyzed as an increase over the initial, undisturbed value.

RESULTS AND DISCUSSION

Typical data from a SST are shown in Fig. 3. The data shown are from the *H* (25.3 kN-124 kPa) treatment at the hardpan depth in the NSL with a hardpan. The value of 0 on the distance axis represents the horizontal location of the wheel axle. Data at positive

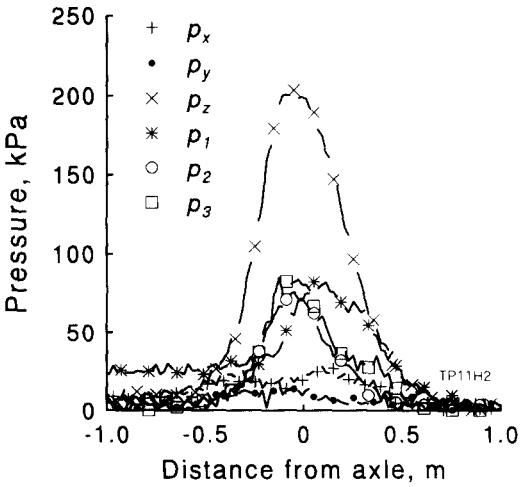

Fig. 3. Typical measured pressures from the stress state transducer under the centerline of the tire.

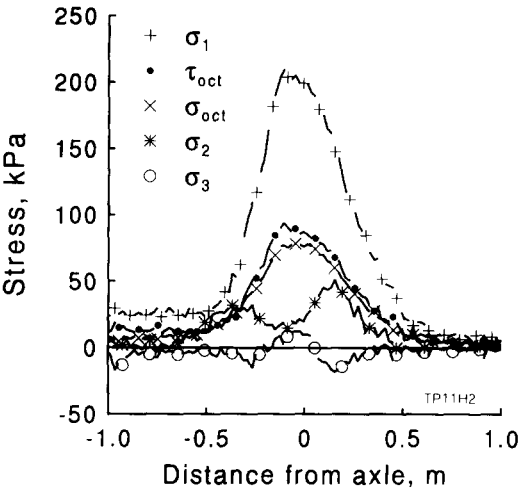

Fig. 4. Calculated stresses from data shown in Fig. 3.

distances represent pressures in front of the wheel axle; data at negative distances represent pressures behind the axle. Figure 4 presents the calculated principal stresses (σ_1, σ_2, and σ_3) and the octahedral stresses (σ_{oct} and τ_{oct}) for the data from Fig. 3 using the same distance axis. The peak values of σ_{oct} and the corresponding values of τ_{oct} were selected for further analyses. Table 3 presents a summary of the means of the four replications of σ_{oct} and τ_{oct} from all treatments, soils and profiles.

The peak values of σ_{oct} and the corresponding values of τ_{oct} were analyzed with SAS [16] using its GLM procedure with its RANDOM and MANOVA multivariate options. The MANOVA option analyzed the two octahedral stresses jointly. Independent variables were soil, profile within soil, depth within soil and profile, dynamic load, inflation pressure and replication within soil and profile. Depth was nested within soil and profile because the SSTs were at different depths in the two soils and profiles. Replication was nested within soil and profile, and profile within soil, because each soil preparation was unique. A summary of the relevant tests of hypotheses for mixed model analysis of variance

Table 3. Mean octahedral stresses at peak σ_{oct} for all treatments

				NSL				DCL			
				Hardpan depth		Shallow depth		Hardpan depth		Shallow depth	
Treatment	Soil profile	Load kN	Inflation pressure kPa	σ_{oct} kPa	τ_{oct} kPa	σ_{oct} kPa	τ_{oct} kPa	σ_{oct} kPa	τ_{oct} kPa	σ_{oct} kPa	τ_{oct} kPa
L	uniform	13.2	41.4	32	32	44	52	34	39	56	79
O	uniform	13.2	124.0	43	55	49	55	53	85	71	108
U	uniform	25.3	41.4	51	55	53	56	84	151	71	104
H	uniform	25.3	124.0	57	54	82	89	91	140	59	70
L	hardpan	13.2	41.4	31	32	51	62	51	86	46	55
O	hardpan	13.2	124.0	39	42	63	51	86	85	65	98
U	hardpan	25.3	41.4	56	52	66	75	84	116	63	75
H	hardpan	25.3	124.0	79	83	106	142	105	177	120	146

Table 4. Hypotheses tests from mixed model analysis of variance

Source	Numerator DF	Numerator MS	Denominator[1] DF	Denominator[1] MS	F-value	Pr > F
			σ_{oct}			
Load	1	24123.1	12	240.1	100.49	0.0001
Ipr[2]	1	9021.6	12	209.3	43.10	0.0001
Load Ipr	1	678.0	12	262.0	2.59	0.1336
Depth (S P)[3]	4	1058.1	48	340.7	3.11	0.0237
Load Depth	4	925.1	48	340.7	2.72	0.0406
Ipr Depth	4	468.8	48	340.7	1.38	0.2564
Ld Ipr Dpth	4	218.1	48	340.7	0.64	0.6364
			τ_{oct}			
Load	1	36517.5	12	1397.6	26.13	0.0003
Ipr	1	19320.9	12	2179.0	8.87	0.0115
Load Ipr	1	270.3	12	1222.3	0.22	0.6466
Depth (S P)	4	4605.2	48	1561.0	2.95	0.0293
Load Depth	4	4508.0	48	1561.0	2.89	0.0320
Ipr Depth	4	857.0	48	1561.0	0.55	0.7006
Ld Ipr Dpth	4	577.1	48	1651.0	0.37	0.2960

[1]Error terms were from SAS PROC GLM; RANDOM/TEST option.
[2]Ipr is inflation pressure.
[3]Depth was nested within soil and profile.

from the RANDOM option of GLM is presented in Table 4. The error terms in Table 4 (denominator) are those determined by the RANDOM option.

Higher levels of either dynamic load or inflation pressure generated higher octahedral stresses beneath the tractor tire in both soils when averaged across all depths and soil profiles. These relationships can be seen in Figs 5 and 6. Both the RANDOM and MANOVA analyses found both dynamic load and inflation pressure to be significant factors (5% level) for the two octahedral stresses. Depth was also a significant factor for both octahedral stresses.

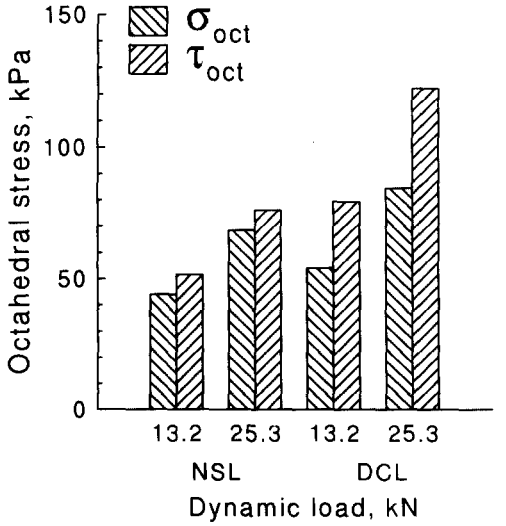

Fig. 5. Effect of dynamic load on octahedral stresses for two soils averaged across profiles and depths.

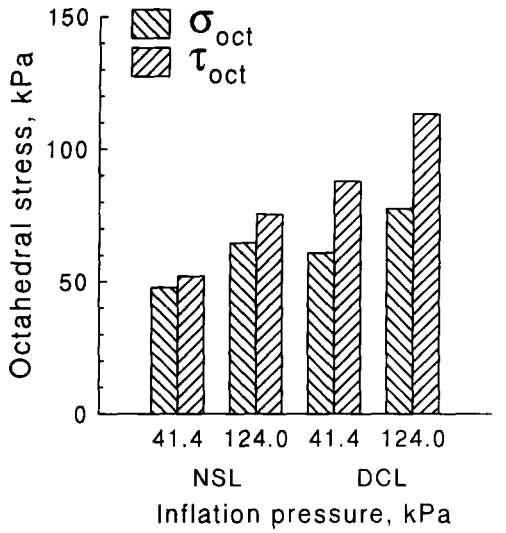

Fig. 6. Effect of inflation pressure on octahedral stresses for two soils averaged across profiles and depths.

Both octahedral stresses displayed a significant interaction between dynamic load and depth (Table 4). The interactions between dynamic load and depth for each soil are shown in Figs 7 and 8. Figure 7 (NSL) shows relationships that are consistent across profile and depth. Figure 8 shows that in the DCL, the stress at the shallow depth in the uniform profile exhibits a trend with dynamic load that is inconsistent with the stresses in the other three depth and soil profile combinations. Similar graphs showed that the octahedral shear stress exhibited the same trends as presented in Figs 7 and 8. Thus, it appears that the source of the significant interaction between dynamic load and depth was just this one profile and depth in the DCL. The authors think that it is safe to ignore these interactions and accept the analysis of the main factors which shows that increases in dynamic load increase soil stresses.

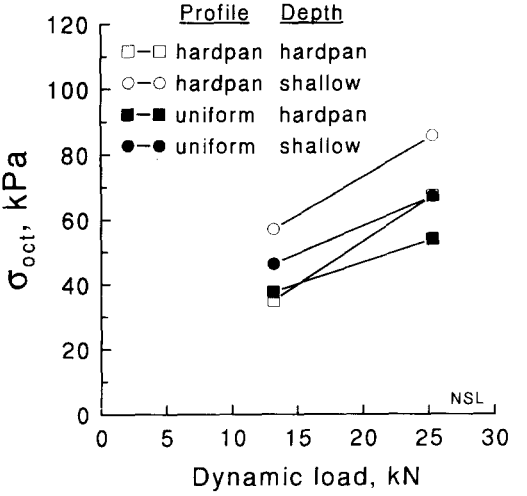

Fig. 7. Effect of dynamic load, depth, and profile in NSL on octahedral normal stress.

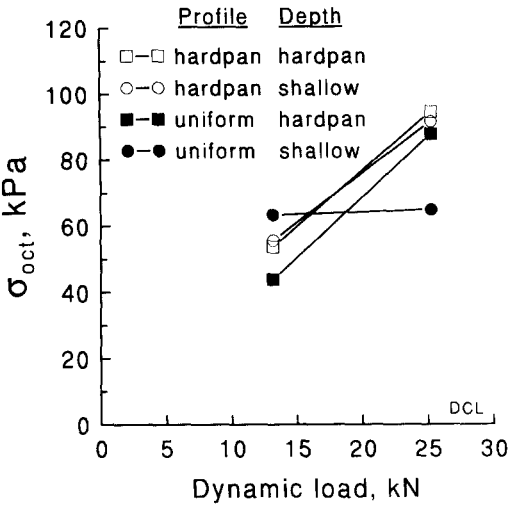

Fig. 8. Effect of dynamic load, depth and profile in DCL on octahedral normal stress.

Table 5. Mean increase in soil bulk density for all treatments

				Increase in bulk density, Mg/m^3			
				NSL		DCL	
Treatment	Soil profile	Load kN	Inflation pressure kPa	Hardpan depth	Shallow depth	Hardpan depth	Shallow depth
L	uniform	13.2	41.4	0.263	0.316	0.096	0.219
O	uniform	13.2	124.0	0.304	0.353	0.175	0.264
U	uniform	25.3	41.4	0.369	0.427	0.248	0.300
H	uniform	25.3	124.0	0.427	0.460	0.258	0.310
L	hardpan	13.2	41.4	0.198	0.280	0.222	0.238
O	hardpan	13.2	124.0	0.250	0.285	0.274	0.296
U	hardpan	25.3	41.4	0.276	0.319	0.317	0.344
H	hardpan	25.3	124.0	0.300	0.371	0.382	0.430

Means of the increase in bulk density are shown in Table 5. The effects of dynamic load and inflation pressure on the increase in bulk density in both soils are shown in Figs 9 and 10. The labels 'hardpan depth' and 'shallow depth' refer to the measurements taken at the 'hardpan' and 'shallow' SST depths. Both dynamic load and inflation pressure significantly influenced (5% level) the increase in bulk density at each depth.

The mean net traction and tractive efficiency data for all treatments in each soil are presented in Table 6. An ANOVA of the net traction and tractive efficiency showed that inflation pressure and dynamic load both had effects on both performance variables, and that higher inflation pressures had lower net traction and tractive efficiencies at the same dynamic load. These results support both the conclusions from the stress and bulk density analyses. Higher inflation pressures at the same dynamic load have lower tractive efficiencies and net tractions, and generate higher soil stresses and soil compaction. Tractive efficiency is lower because energy is expended in compacting the soil.

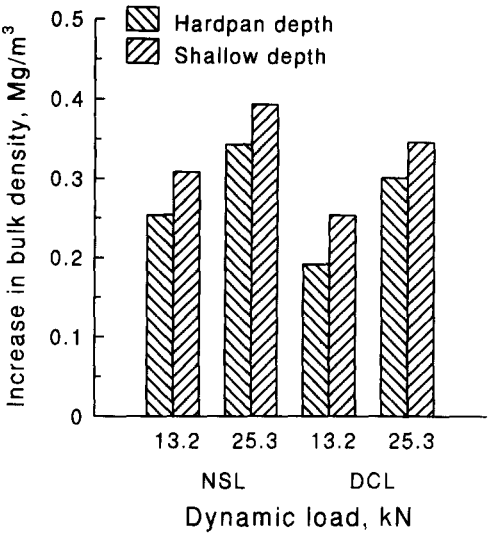

Fig. 9. Effect of dynamic load on increases in bulk density for two soils averaged across profiles.

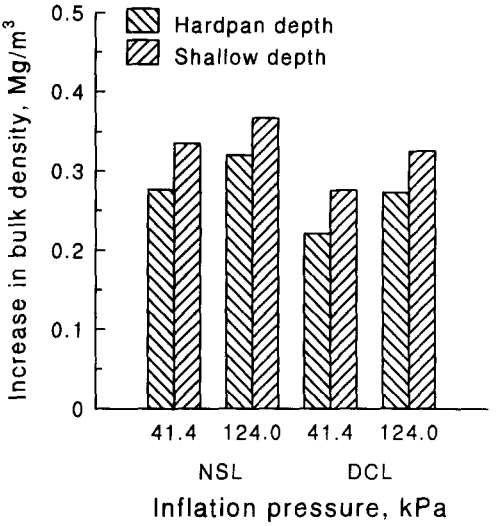

Fig. 10. Effect of inflation pressure on increase in bulk density for two soils averaged across profiles.

Table 6. Mean tractive performance data

			NSL		DCL	
Treatment	Load kN	Inflation pressure kPa	Net traction kN	Tractive efficiency %	Net traction kN	Tractive efficiency %
L	13.2	41.4	5.4	67.4	5.7	69.8
O	13.2	124.0	3.9	58.4	4.3	63.6
U	25.3	41.4	11.6	68.7	12.7	73.4
H	25.3	124.0	8.3	62.0	8.9	66.5

CONCLUSIONS

Stress state transducers were placed at two depths beneath the centerline of the path of the tractor tire in two different profiles in each of two soils. The tire was operated at two different levels of rated load taken from the tire manufacturer's published load tables, and at two other combinations of load and inflation pressure representing over-inflated and under-inflated conditions. This experiment showed that:

(1) increasing dynamic load at a constant inflation pressure increased soil stresses and soil bulk density; and

(2) increasing inflation pressure at a constant dynamic load increased soil stresses and soil bulk density, and decreased net traction and tractive efficiency.

A corollary of conclusion (2): inflation pressure should be set at the manufacturer's recommendation for the actual load on the tire, which is the minimum acceptable inflation pressure for that load. This will minimize soil stresses and compaction, and maximize efficiency.

Acknowledgment—The authors wish to acknowledge the technical contributions of Deere and Company, and The Goodyear Tire and Rubber Company.

REFERENCES

1. Firestone, Maximize tractive performance of radial rear tractor tires with proper inflation. Bridgestone/Firestone, INC, February 1992.
2. Goodyear, Optimum tractor tire performance handbook. The Goodyear Tire & Rubber Company, January 1992.
3. Deere, J., "New" radial tire inflation pressure recommendations. *Tractor Talk* February 1992.
4. Reichenberger, L., Radial tires need "cheeks". *Farm Journal* (reprint). February 1992.
5. Wiley, J. C., Romig, B. E., Anderson L. V. and Zoz, F. M., Optimizing dynamic stability and performance of tractors with radial tires. ASAE Paper No. 92-1586, ASAE, St. Joseph, MI 49085 1992.
6. Burt E. C. and Bailey, A. C., Load and inflation pressure effects on tires. *Trans. ASAE*, 1982, **25** (4), 881–884.
7. Soane, B. D., Blackwell, P. S., Dickson, J. W. and Painter, D. J., Compaction by agricultural vehicles: a review II. Compaction under tyres and other running gear. *Soil and Tillage Res.*, 1980, **1** (4), 373–400.
8. Bailey, A. C., Burt, E. C., Wood, R. K. and Johnson, C. E., The effects of tire dynamic load on soil stress states. *ASAE Paper No.* 88–1511, 1988, ASAE, St. Joseph, MI 49805.
9. Bailey, A. C., Raper, R. L. and Burt, E. C., The effects of tire inflation pressure on soil stress states. *ASAE Paper No.* 91-1062, 1991, ASAE, St. Joseph, MI 49085.
10. Bailey, A. C., Burt, E. C., Raper, R. L. and Monroe, G. E., Tire-generated stress states above a hard pan. *ASAE Paper No.* 89-1098, 1989, ASAE, St. Joseph, MI 49085.
11. Nichols, T. A., Bailey, A. C., Johnson, C. E. and Grisso, R. D., A stress state transducer for soil. *Trans. ASAE*, 1987, **30** (5), 1237–1241.
12. Bailey, A. C. and Burt, E. C., Soil stress states under various tire loadings. *Trans. ASAE* 1988, **31** (3), 672–676, 682.
13. Burt, E. C., Reaves, C A., Bailey, A. C. and Pickering, W. D., A machine for testing tractor tires in soil bins. *Trans. ASAE* 1980, **23** (3), 546–547, 552.
14. Lyne, P. W. L., Burt, E. C. and Jarrell, J. D., Computer control for the National Tillage Machinery Laboratory single wheel tester. *ASAE Paper No.* 83-1555, 1983, ASAE, St. Joseph, MI 49085.
15. Bailey, A. C., Raper, R. L., Way, T. R., Burt, E. C. and Johnson, C. E., Soil stresses under tractor tires at various inflation pressures. *Proc. 11th Int. Conf. of the ISTVS* 1993, Lake Tahoe, NV, U.S.A.
16. SAS. SAS/STAT User's Guide, Version 6, 4th edition. SAS Institute, Inc. Cary, NC, U.S.A. 1990.